Published in final edited form as:
Am J Physiol Regul Integr Comp Physiol. 2016 August 1; 311(2): R254–R262. doi:10.1152/ajpregu.00154.2016.

Components of the cannabinoid system in the dorsal periaqueductal gray are related to resting heart rate

Caron Dean[1,3], **Cecilia J. Hillard**[2], **Jeanne L. Seagard**[1,3], **Francis A. Hopp**[3], and **Quinn H. Hogan**[1,3]

[1]Department of Anesthesiology, Medical College of Wisconsin, Milwaukee, Wisconsin

[2]Department of Pharmacology, Medical College of Wisconsin, Milwaukee, Wisconsin

[3]Zablocki Veterans Affairs Medical Center, Milwaukee, Wisconsin

Abstract

The present study was undertaken to examine whether variations in endocannabinoid signaling in the dorsal periaqueductal gray (dPAG) are associated with baseline autonomic nerve activity, heart rate, and blood pressure. Blood pressure was recorded telemetrically in rats, and heart rate and power spectral analysis of heart rate variability were determined. Natural variations from animal to animal provided a range of baseline values for analysis. Transcript levels of endocannabinoid signaling components in the dPAG were analyzed, and endocannabinoid content and catabolic enzyme activity were measured. Higher baseline heart rate was associated with increased anandamide content and with decreased activity of the anandamide-hydrolyzing enzyme and fatty acid amide hydrolase (FAAH), and it was negatively correlated with transcript levels of both FAAH and monoacylglycerol lipase (MAGL), a catabolic enzyme for 2-arachidonoylglycerol (2-AG). Autonomic tone and heart rate, but not blood pressure, were correlated to levels of FAAH mRNA. In accordance with these data, exogenous anandamide in the dPAG of anesthetized rats increased heart rate. These data indicate that in the dPAG, anandamide, a FAAH-regulated lipid, contributes to regulation of baseline heart rate through influences on autonomic outflow.

Keywords

endocannabinoids; heart rate; sympathetic nerve activity; dorsal periaqueductal gray; rat

WHILE THE DEBATE ON THE HEALTH benefits and risks of cannabis use continues, ongoing research highlights the diverse physiological and pathophysiological actions mediated by the endogenous cannabinoid (endocannabinoid) system (17, 31). The endocannabinoid system is

Address for reprint requests and other correspondence: C. Dean, Dept. of Anesthesiology, Research Service 151, Zablocki VA Medical Center, Milwaukee WI 53295 (cdean@mcw.edu).

DISCLOSURES

No conflicts of interest, financial or otherwise, are declared by the authors.

AUTHOR CONTRIBUTIONS

C.D., C.J.H., J.L.S., F.A.H., and Q.H.H. conception and design of research; C.D., C.J.H., and J.L.S. performed experiments; C.D., C.J.H., and F.A.H. analyzed data; C.D., C.J.H., J.L.S., F.A.H., and Q.H.H. interpreted results of experiments; C.D., F.A.H., and Q.H.H. prepared figures; C.D. drafted manuscript; C.D., C.J.H., J.L.S., F.A.H., and Q.H.H. edited and revised manuscript; C.D., C.J.H., J.L.S., F.A.H., and Q.H.H. approved final version of manuscript.

composed of the endocannabinoids, their metabolic and catabolic enzymes, their G protein-coupled cannabinoid 1 and 2 receptors (CB_1R and CB_2R) and putative membrane transporters. There are two endogenous ligands, *N*-arachidonylethanolamine (anandamide or AEA) (16) and 2-arachidonoylglycerol (2-AG) (39, 53) whose concentrations are closely regulated by endocannabinoid-hydrolyzing enzymes, which, in turn, influence signaling. In the brain, the majority of anandamide is hydrolyzed to arachidonic acid and ethanolamine by fatty acid amide hydrolase (FAAH) (9), while 2-AG undergoes hydrolysis primarily through monoacylglycerol lipase (MAGL) (4). In addition, endocannabinoid signaling is also modulated by altered CB_1R density, which can be regulated through changes in agonist availability, mRNA processing, turnover, or transcription (7, 11, 18). CB_1Rs are especially abundant in the central nervous system, but are also expressed in postganglionic nerve terminals (44). CB_2Rs are found in the brain (57) but are predominant in immune cells (20), while both receptors have been identified in the myocardium (1, 41) The ubiquity of cannabinoid receptors undoubtedly contributes to the complexity of responses evoked by systemic administration of cannabinoids.

The cardiovascular effects of systemically administered cannabinoid agonists appear to be dominated by peripheral actions. Typically, systemic administration of cannabinoids evokes a depressor and bradycardic response (32, 35, 58), attributed, in part, to activation of peripheral CB_1Rs on autonomic nerves innervating the heart and on sympathetic nerves innervating the vascular smooth muscle. Yet, in humans, the prominent and most consistent response to the cannabinoid Δ^9-tetrahydrocannabinol (THC) is a CB_1R-dependent increase in heart rate (25, 30). This tachycardia, which is usually accompanied by a small increase in blood pressure and an increase in cardiac output, is attributed to an increase in cardiac sympathetic nerve activity and a decrease in cardiac parasympathetic nerve activity (2). While there is evidence for the involvement of peripheral CB_1Rs in the increase in heart rate (30, 55), many studies support a centrally mediated contribution (3, 27, 43). Recent studies suggest that central administration of cannabinoids primarily evokes a sympathoexcitatory and vagal inhibitory response mediated by CB_1Rs. Specifically, cannabinoids administered into the cisterna magna (ic) of conscious rabbits elicits an increase in renal sympathetic nerve activity, plasma norepinephrine, and blood pressure accompanied by vagally mediated bradycardia (42), which are sensitive to CB_1R blockade, with similar responses identified in anesthetized rats (50). Directed microinjections of cannabinoids into the rostroventrolateral medulla (RVLM), a component of descending pathways for sympathetic outflow, also increases blood pressure and splanchnic sympathetic nerve activity through CB_1R activation, demonstrating a central influence of endocannabinoid signaling on cardiovascular parameters (45). Cannabinoids can enhance autonomic activity and cardiovascular parameters through endocannabinoid signaling in the dorsal periaqueductal gray (dPAG), a highly integrative region, the activation of which is associated with enhanced sympathetic and cardiovascular regulation in emotional behaviors (28). Endocannabinoids function in the dPAG by inhibiting tonically active GABAergic neurons to exert a profound activation of output neurons, leading to an increase in sympathetic nerve activity and blood pressure (12, 13).

Evidence for the role of dPAG neurons in regulation of baseline cardiovascular parameters is inconclusive, as lesion studies failed to provide basal heart rate and blood pressure data (33,

34, 52). While endocannabinoid modulation of sympathetic outflow is associated with stress responses in the dPAG, (12, 13), it is not known whether endocannabinoids in this midbrain region contribute to ongoing sympathetic tone through this circuitry, Therefore, the present study was undertaken to determine whether endocannabinoid signaling in the dPAG contributes to autonomic and cardiovascular regulation under resting conditions.

MATERIALS AND METHODS

Animals

The protocol for this study was approved by the Animal Care and Use Committees at the Medical College of Wisconsin and the Zablocki Veterans Affairs Medical Center.

Chronic Studies

Radiotelemetry—All rats (male Sprague-Dawley, 320–330 g) were implanted with a PA-C10 transmitter [Data Sciences International (DSI), St. Paul, MN] to telemetrically monitor arterial blood pressure. Rats were anesthetized with isoflurane (5% induction, 1.75–2% maintenance) in O_2, and the cannula (0.43 mm outer diameter polyethylene) attached to the transmitter was inserted into the left femoral artery through a small inguinal incision, with care taken to avoid manipulation of the adjacent femoral nerve. The transmitter was fixed in a subcutaneous pocket on the left flank of the rat, and the incision was closed with 3-0 silk suture. Animals were treated with carprofen (5 mg/kg sc) at the start of surgery and on *day 1* post op. Resting blood pressure was monitored in freely moving conditions from 7–9 AM on *days 5–7* after implantation surgery. Blood pressure recordings were obtained during times of minimal movement to avoid the elevated pressure that accompanies activity.

Tissue Collection

On *day 7*, after the blood pressure monitoring period, animals were deeply anesthetized with isoflurane (5%) in O_2 and decapitated. The brain was removed and the dorsal region of the PAG, the length of the cerebral aqueduct, was quickly excised. Under a microscope, the PAG tissue was dissected at the lateral and dorsal borders of the periaqueductal gray matter and a ventral cut was made at the mid-cerebral aqueduct. Though there are no anatomical distinctions of PAG columns, the dissected tissue sample should be limited to the dPAG, which includes the dorsal, dorsomedial, and dorsolateral columns. Tissue samples were frozen in liquid nitrogen and stored at −80°C until analysis.

dPAG tissue was analyzed for either *1*) mRNA levels of components of the cannabinoid system, *2*) FAAH and MAGL activity, or *3*) endocannabinoid content.

Real-time RT-PCR—Expression levels of mRNA were measured for a panel of components of the cannabinoid system in the dPAG, using standard techniques. Total RNA was extracted from each dPAG sample using RNeasy Mini kit (Qiagen, Valencia CA). cDNA was synthesized using iScript reverse transcriptase (Bio-Rad, Hercules CA). mRNA was quantified using SYBR-Green as the detection agent, and amplifications were performed with the Eppendorf Mastercycler Realplex in 25-μl reaction volumes containing cDNA, primers, and iQ Supermix (Bio-Rad). Thermal cycling proceeded with one

amplification cycle of denaturation at 95°C for 2 min, followed by 45 cycles of 95°C for 15 s, 55°C for 15 s, and 68°C for 20 s. The cycle at which amplification reached threshold (C_T) was determined for each amplicon. All reactions were performed in duplicate. Results were calculated by subtracting C_T of hypoxanthine guanine phosphoribosyltransferase (HPRT) as a baseline control (ΔC_T) and normalized to $200^{-\Delta C_T}$. Specificity of the RT-PCR reaction was confirmed by melting curves. Efficiencies were 0.9–1.1 for each amplicon.

The following sequence-specific primers were used, listed as 5′ to 3′: HPRT forward: GCA GAC TTT GCT TTC CTT GG and reverse: CCG CTG TCT TTT AGG CTT TG; FAAH forward: GAG GCT GGC TTT CAA CTC AC and reverse: TTC GGA AGA CAG GCC AAT AC; MAGL forward: CAC CTC TGA TCC TTG CCA AT and reverse: GAT GAG TGG GTC GGA GTT GT; and CB_1R forward: TCA GCA AGA AGT CAT CAG TAA GAG and reverse: CCA CCA TCC TCC ACA CTC C.

Enzyme activity assays—Enzyme activity assays were performed on dPAG tissue from a separate group of animals ($n = 19$). Frozen dPAG tissue samples were weighed and homogenized in 10 volumes TME buffer (50 mM Tris·HCl, pH 7.4; 3 mM $MgCl_2$, and 1 mM EDTA). Homogenates were centrifuged at 12,000 rpm for 20 min at 4°C. The supernatant of cytosolic protein was reserved for MAGL activity assay. The pellet containing a crude membrane fraction for FAAH activity assay was resuspended in 10 volumes TME buffer. Protein concentrations were determined by the Bradford method (Bio-Rad, Hercules, CA). Samples were frozen at −80°C until assayed.

FAAH Activity Assay

FAAH activity was measured as the conversion of anandamide labeled with [^{3}H] in the ethanolamine portion of the molecule ([^{3}H]AEA; 60 Ci/mmol; American Radiolabeled Chemicals, St. Louis, MO), [^{3}H]AEA to [^{3}H]ethanolamine, as reported previously (5). Membranes from each sample (0.9 mg protein) were incubated in TME buffer (0.5 ml) containing 1.0 mg/ml fatty acid-free BSA and 0.2 nM [^{3}H]AEA. A duplicate incubation was carried out in the presence of the FAAH inhibitor URB597 (cyclohexylcarbamic acid 3′-carbamoylbiphenyl-3-yl ester; 1 μM) (Tocris Bioscience, Minneapolis MN) to determine non-FAAH-mediated hydrolysis that was subtracted from the total hydrolysis. Hydrolysis occurred for 10 min at 30°; the incubations were stopped with the addition of 2 ml chloroform/methanol (1:2). After standing on ice for 30 min with regular vortexing, 0.67 ml chloroform and 0.6 ml water were added. Aqueous and organic phases were separated by centrifugation at 2,500 rpm for 5 min. The amount of [^{3}H] in 500 μl of the aqueous phase was determined by liquid scintillation counting, and the conversion of [^{3}H]AEA to [^{3}H]ethanolamine was calculated and normalized to the amount of membrane protein.

Assay for Cytosolic Hydrolysis of 2-Oleoyl[^{3}H]Glycerol (2-OG)

Because the glycerol esters of oleic acid and arachidonic acid are hydrolyzed by MAGL with similar catalytic efficiency (24) and because 2-OG, but not 2-AG, is currently available radiolabeled in the glycerol moiety, 2-oleoyl[^{3}H]glycerol ([^{3}H]2-OG; 60 Ci/mmol; American Radiolabeled Chemicals, St. Louis MO), was used to estimate the activity of the hydrolytic enzymes (primarily MAGL) involved in the catabolism of 2-AG, as reported

previously (51). Cytosolic protein was used for this assay, and all incubates included 1 μM URB-597. Non-MAGL-mediated hydrolysis of 2-OG was assessed in the presence of the specific MAGL inhibitor, 30 μM JZL184 (4-[*Bis*(1,3-benzodioxol-5-yl)hydroxymethyl]-1-piperidinecarboxylic acid 4-nitrophenyl ester) (Tocris Bioscience) and was subtracted from the total hydrolysis. Otherwise, the assay was carried out identically to the assay for FAAH.

Lipid measurement—Lipids were analyzed in dPAG tissue from a separate group of animals ($n = 10$). For analysis of the content of the *N*-acylethanolamines (NAEs), anandamide, *N*-oleoylethanolamine (OEA), and *N*-palmitoylethanolamine (PEA), and the O-acylglycerols, 2-AG and 2-OG. dPAG samples were subjected to a lipid extraction process, as described previously (46). Briefly, tissue samples were weighed and homogenized in acetonitrile containing 34 pmol of [$^2H_8$]AEA and 66 pmol of [$^2H_8$]2-AG for extraction. Tissue was homogenized, sonicated for 30 min, and incubated overnight at −20°C to precipitate the proteins. Particulates were removed from acetonitrile by centrifugation at 1,500 rpm, the supernatants were removed and evaporated to dryness under N_2 gas, and the extracted lipids were resuspended in methanol and stored at −80°C until analysis.

The content of anandamide, its structural analogs OEA and PEA and 2-AG and its analog 2-OG within lipid extracts in methanol from dPAG tissue were quantified using isotope-dilution liquid chromatography-mass spectrometry, as described previously (47, 49). Samples (5 μl) were separated on a reverse-phase C18 column (Kromasil, 250 × 2 mm, 5 μm diameter) using mobile phase A (deionized water, 1 mM ammonium acetate, and 0.005% acetic acid) and mobile phase B (methanol, 1 mM ammonium acetate, and 0.005% acetic acid). Samples were eluted at 300 μl/min using a linear gradient of 85% solvent B to 90% solvent B over 15 min. Selective ion monitoring, made in the positive ion mode, was used to detect [$^2H_8$]AEA (*m/z* 356), AEA (*m/z* 348), OEA (*m/z* 326), PEA (*m/z* 300), [$^2H_8$]2-AG and 1(3)-AG (*m/z* 387), 2-AG, and 1(3)-AG (*m/z* 379), and 2-OG and 1(3)-OG (*m/z* 357). Lipid contents were normalized to tissue wet weight.

Acute microinjection study—Male Sprague-Dawley rats (350–390 g) were anesthetized with pentobarbital sodium (50 mg/kg ip), and a catheter was inserted into a femoral vein for subsequent administration of anesthetic, as necessary to block the toe pinch reflex in unparalyzed animals (supplemental doses 2 mg/kg iv). Arterial blood pressure was monitored continuously from a cannula inserted into a tail artery, connected via a pressure transducer to a computer-based data acquisition and storage system (Apple Macintosh G4 computer, AD Instruments PowerLab/8SP with chart software). The trachea was cannulated for ventilation with room air (Harvard 683 respirator) after administration of pancuronium bromide (0.1 mg/kg iv, with supplemental doses 0.05 mg/kg). A heating pad was used to maintain body temperature at 37°C. The head of the animal was fixed in a stereotaxic frame (Kopf, Tujunga CA), and the activity of a renal nerve, which was exposed retroperitoneally and positioned on flexible silver wire electrodes, was recorded. The electrophysiological signal was directed to high-impedance differential amplifiers (gain = 1,000; 0.1–10-kHz passband), followed by filter/amplifiers (gain up to 400; high- and low-pass filtering 10 Hz to 3 kHz) and displayed online. Heart rate was derived from blood pressure and recorded on

the computer-based data acquisition system along with the arterial blood pressure and renal sympathetic nerve activity.

A dorsal craniotomy was performed, and the dura was reflected to allow the insertion of a glass micropipette for pressure ejection of the CB_1 receptor agonist anandamide diluted in 0.01% Tocrisolve100 (50 μM; Tocris Cookson, St. Louis, MO). The micropipette was advanced into the midbrain slowly using a microdrive, targeting the dPAG. The volume of injectate was measured by observing the level of the fluid meniscus through a graduated monocular microscope eyepiece (7 nl/div). Blood pressure and renal sympathetic nerve data was published previously (12, 13).

Data and Statistical Analyses

Chronic studies—Resting blood pressure data were analyzed for heart rate and heart rate variability (HRV) using the DSI Dataquest A.R.T. software system. Power spectral analysis of heart rate was used to determine HRV from blood pressure data, as described previously (21). A cubic algorithm was used to interpolate blood pressure data sampled at 500 Hz to 2 kHz. The blood pressure data were used to calculate an inter-beat interval (IBI) series from three 5-min segments, each with five overlapping (50%) subsegments of 512 points. The IBI was converted into an instantaneous heart rate using the formula: heart rate (beats/min) = 60/IBI (s). The IBI values were then interpolated at 50 Hz (cubic algorithm) and detrended; then, the mean was suppressed to create the data points equally spaced in time for further analysis. The power was calculated for each data set over the frequency ranges of 0.25–1 Hz (low frequency, LF) and 1–3 Hz (high frequency, HF), with the results from the three segments averaged for the final determination of density within each frequency band. LF and HF powers were normalized and expressed as percentages of total power (LF + HF powers), and the LF/HF ratio was calculated from these values.

Power spectral analysis determination of HRV provided values for LF and HF powers as a percentage of total power and the LF/HF power ratio. Although HF power is generally accepted as a reflection of vagal modulation of heart rate (19, 36), the LF power may not be an accurate representation of sympathetic modulation of heart rate. A significant amount of power in the LF band is thought to be due to vagal contributions, and therefore, the LF power/HF power ratio is thought to represent the sympathovagal balance (19). An increase in the LF power/HF power ratio indicates a change to a relatively higher sympathetic versus vagal cardiac modulation, while a decrease in the LF power/HF power ratio reflects the opposite.

Real-time RT-PCR—Blood pressure, heart rate, and HRV values were calculated for each daily monitoring period. The values were averaged to provide a baseline value for heart rate, HF power, LF power/HF power ratio, and mean arterial blood pressure for each animal, which were plotted against transcript levels of FAAH, MAGL, and CB_1Rs. Linear regression analyses were performed in SigmaPlot 11 (Systat Software, San Jose CA) to evaluate potential associations. Significance was set at the 0.05 level. Heart rate data for the PCR group of animals were tested for normality using Shapiro-Wilk test.

Enzyme assays and lipid measurement—Animals for enzyme assays and endocannabinoid content were grouped by baseline heart rate into either a high category (>350 beats/min) or a low category (<350 beats/min), using a threshold derived from a prior study (21). Unpaired *t*-tests were performed between the heart rate categories on anandamide and 2-AG content, and FAAH and MAGL activity, with the level of significance set at <0.05. Correlations between baseline heart rate and dPAG content of anandamide, 2-AG, and their structural analogs were evaluated through linear regression analyses with significance set at <0.05.

Acute microinjection study—For the acute study, heart rate was calculated for 10-s periods, and baseline heart rate prior to anandamide microinjections was compared with peak heart rate response using a *t*-test with significance set at the 0.05 level.

RESULTS

Baseline Heart Rate and HRV

For animals in the real-time RT-PCR group ($n = 34$), the baseline heart rates ranged from 300 to 404 beats/min, with a normal distribution and a mean of 345 beats/min. In the present study, autonomic components of heart rate were determined by power spectral analysis of HRV. High-frequency power showed a significant negative correlation with LF power/HF power ratio ($R^2 = -0.713$) (Fig. 1*A*). The LF power/HF power ratio was used as an indicator of sympathovagal balance and demonstrated a positive correlation with heart rate (Fig. 1*B*), while the HF power, an indicator of parasympathetic tone, had a negative correlation with heart rate (Fig. 1*C*). These data indicate that increased sympathetic activity and lower parasympathetic tone accompany higher-baseline heart rates.

Real-time RT-PCR—mRNA expression of components of endocannabinoid signaling in the dPAG was analyzed by real-time RT-PCR. The correlation coefficient values for the FAAH, MAGL, and CB_1R mRNA transcript levels, and autonomic and cardiovascular parameters are shown in Table 1. The data demonstrate a modest, but significant, negative correlation between expression of the endocannabinoid hydrolyzing enzymes FAAH ($R^2 = -0.117$) (Fig. 2*A*) and MAGL ($R^2 = -0.149$) (Fig. 2*B*) and heart rate, suggesting that the reduced degradation of endocannabinoids could increase heart rate.

Enzyme assays—Endocannabinoid enzyme assays performed on the dPAG of animals in the high heart rate category [mean 364 beats/min (SD) ± 14.5; $n = 9$] compared with the low heart rate group [321 beats/min (SD) ± 10.0; $n = 10$] (Fig. 3*A*) demonstrate a significant reduction in FAAH activity (1.9 vs. 0.45 fmol ethanolamine formed per minute per milligram protein; $P < 0.01$) in the high heart rate group (Fig. 3*B*), while the corresponding decrease in MAGL activity was not significant between the groups (11.2 vs. 6.7 fmol of glycerol formed per minute per milligram protein) (Fig. 3*C*). These data predict that endocannabinoid content, primarily anandamide, in the dPAG should show a positive correlation with heart rate.

Lipid measurement—To test this, in a third set of animals, endocannabinoid content in the dPAG was compared in animals with high heart rates (>350 beats/min; $n = 6$) to those

with low heart rates (<350 beats/min; $n = 4$). The mean heart rates for the two groups were significantly different, 328 beats/min (SD ± 7.1) vs. 394 beats/min (SD ± 12.0) (Fig. 4*A*). Anandamide content in the dPAG was significantly lower ($P < 0.002$) in the low-heart rate group (252.6 fmol/mg; SD ± 27.6) compared with the high-heart rate group (352.4 fmol/mg; SD ± 39.6) (Fig. 4*B*). In contrast, there was no significant difference in 2-AG content between the two groups (low-heart rate group, 37.8 pmol/mg; SD ± 7.3; high-heart rate group, 40.5 pmol/mg; SD ± 13.9) (Fig. 4*C*). Regression analyses demonstrated a significant correlation between baseline heart rate and the dPAG content of anandamide, with an R^2 value of 0.597, but no correlation with OEA and PEA substrates for FAAH, or with 2-AG and 2-OG (Fig. 5).

Transcript Levels and HRV

We found a significant positive correlation between FAAH expression and HF power and negative correlation between FAAH and the ratio of LF/HF power (Table 1), suggesting that low dPAG anandamide levels were associated with higher parasympathetic tone, lower sympathetic tone, and consequently lower heart rate. There was no evidence for a correlation between MAGL transcript levels and components of HRV (Table 1). In addition, there was no correlation between mRNA expression of CB1 receptors in the dPAG and heart rate, autonomic parameters, or blood pressure (Table 1). Finally, there was no correlation between transcript levels of any endocannabinoid signaling components and blood pressure (Table 1).

Acute microinjection study—In anesthetized rats, microinjection of anandamide (35 nl, 1.75 pmol) that are limited to sites in the dPAG can elicit an increase in sympathetic nerve activity (+35.5 ± 7.1%) and blood pressure (+11 ± 2 mmHg) (12, 13). In 31 animals, sympathoexcitatory and pressor responses to anandamide microinjection in the dPAG were accompanied by increases in heart rate (Fig. 6A). The heart rate evoked by anandamide was significantly higher than baseline ($P = 0.03$) (Fig. 6*B*), increasing by up to 44 beats/min with a mean increase of 17.1 (± 2.2 beats/min) (Fig. 6*C*). Although there was a wide range of responses, there was no topographical organization to the magnitude of the responses, except that all sites were within the dPAG region, as reported previously for sympathetic and blood pressure responses (12, 13). The anandamide-evoked increases in heart rate were evident despite an anesthesia-related increase in baseline heart rate (413 beats/min in anesthetized animals vs. 345 beats/min in the chronic unanesthetized group of rats) (36, 39).

DISCUSSION

Baseline heart rates vary widely in rats, as they do in humans. The present data indicate that the activity of FAAH, which is a primary regulator of the endocannabinoid anandamide, in the dPAG influences baseline heart rate and the underlying autonomic activity. As heart rate was not correlated to transcript levels of CB_1Rs, these data also suggest that endocannabinoid signaling is regulated by hydrolyzing enzyme control of endocannabinoid content, rather than by shifts in CB_1R expression. We also show potential differential roles for the specific endocannabinoids, with a greater contribution from anandamide than 2-AG. In agreement with previous studies, heart rate is correlated to LF/HF power ratio of HRV and negatively correlated to HF power, indicating elevated sympathovagal balance with

increased heart rate (21). The microinjection data demonstrate that increases in heart rate are elicited by anandamide in the dPAG, accompanied by increased renal sympathetic nerve activity (12, 13). The evoked pressor response suggests that an increase in cardiac sympathetic, or decrease in parasympathetic activity, was also induced. These data provide a central nervous system site of endocannabinoid signaling that influences autonomic activity and heart rate and suggests a central site of action for the tachycardic effects of THC.

Anandamide content in the dPAG is significantly higher in rats with higher baseline heart rates, which is supported by a negative correlation between levels of expression of FAAH mRNA and heart rate, and decreased FAAH enzyme activity at higher heart rates. Thus, the present data suggest that FAAH expression in the dPAG affects the autonomic balance with an increased vagal contribution at lower heart rates combined with a decreased sympathovagal balance. The significant relationships that we found between heart rate and both FAAH and MAGL transcript levels support endocannabinoid signaling as a contributing factor in control of the resting hemodynamic state.

FAAH, a membrane protein expressed primarily in large outflow neurons, hydrolyzes anandamide to arachidonic acid and ethanolamide, a catabolic process that is integral to the regulation of anandamide concentrations in the brain (8, 56). In addition to the NAEs, FAAH also hydrolyzes oleamide and N-acyltaurines, with a minor role in 2-AG hydrolysis in vivo (9, 49). Although FAAH catabolizes families of lipids that have targets other than the CB_1R (22), the finding that anandamide content but not that of OEA, PEA, 2-AG, or 2-OG, correlates to baseline heart rate suggests that FAAH enzyme activity in the dPAG contributes to regulation of basal heart rate specifically through alteration of anandamide content. Further studies are required to demonstrate that the correlations identified are the result of CB_1R activation. In addition, there are many factors influencing autonomic activity and heart rate, and the moderate values that we observed for the correlation coefficients of heart rate with FAAH and MAGL indicate that there are other determinants of baseline heart rate. Blood pressure was not correlated to FAAH activity or expression or anandamide concentrations in the dPAG, which is not surprising, as it is tightly buffered by neuronal circuitry in other central cardiovascular regions, primarily the nucleus tractus solitarius.

Central administration of cannabinoids has been shown to enhance sympathetic nerve activity, blood pressure, and plasma noradrenaline (12, 13, 42, 45, 50), but the site of action is unknown. Data suggest the midbrain dPAG as a potential site of action, as it influences sympathetic outflow to coordinate specific patterns of cardiovascular events similar to those elicited by local microinjection of cannabinoids (12–15, 45). Neurons in the dPAG receive descending inputs from the hypothalamus to coordinate the autonomic and cardiovascular components of the response to stress, which consist primarily of an increase in visceral sympathetic nerve activity, heart rate, and blood pressure (23). We have shown that CB_1Rs in the dPAG modulate the sympathoexcitatory and pressor responses from hypothalamic stimulation and that activation of CB_1Rs in the dPAG enhances sympathetic nerve activity and blood pressure (12, 13). Stress-related dPAG neurons are also under heavy tonic GABAergic inhibition that, when released, increases sympathetic outflow (10, 13), a function performed by endocannabinoids (13). Taken together, these data indicate a role for endocannabinoid signaling in facilitating sympathetic nervous system function in stress

pathways of the dPAG. Data from the present study suggest that there may be a physiological role for this neuronal circuitry.

Individual stress levels, largely determined by genetic and environmental influences, are higher in some subjects than others (26, 38). Lability of activity in neuronal networks of the dPAG driven by ongoing levels of stress, could influence release of endocannabinoids to modulate autonomic output and heart rate (54). Endocannabinoids are mobilized by enhanced excitatory synaptic input, so the prevailing level of activity in the dPAG could influence their release and contribute to the fine-tuning of physiological levels of autonomic activity and heart rate, relative to the ongoing stress levels, defined uniquely for an individual. In support of this, there is evidence that endocannabinoids are released in the central nervous system under normal conditions. Brown et al. (6) demonstrated that brief bursts of synaptic activity, typical of ongoing patterns evident at many central synapses are sufficient to produce endocannabinoid-mediated retrograde inhibition. Functional evidence for this was presented by Patel et al. (48) who observed a dose-dependent increase in serum corticosterone upon administration of the CB_1R antagonist SR141716, which suggests a tonic inhibition of the hypothalamic-pituitary-adrenal axis. From the present data, CB_1R blockade in the dPAG might then be expected to uncover ongoing endocannabinoid release, but a dose that attenuated anandamide-evoked sympathoexcitation does not alter baseline sympathetic nerve activity or blood pressure (12). Perhaps a more widespread inhibition, beyond the limited diffusion of nanoliter volumes of injectate, is required to alter baseline parameters. Anandamide has been implicated as a key contributor to endocannabinoid tone. Activity deprivation at hippocampal synapses enhances GABAergic inhibition and increases FAAH activity leading to reduced anandamide tone, without affecting 2-AG signaling (29). Our findings provide a potential functional role for anandamide in the dPAG in fine-tuning synaptic regulation of autonomic nerve activity.

Perspectives and Significance

The present study suggests a novel modulatory contribution for the endocannabinoid system in the dPAG in the setting of baseline heart rate through autonomic changes. The components required for endocannabinoid regulation of autonomic activity and heart rate are all present in the dPAG. Data show activity and expression of catabolic enzymes that regulate endocannabinoid content and, therefore, signaling in the dPAG can influence baseline heart rate through autonomic adjustments. This mechanism may be an example of synaptic plasticity, since endocannabinoid signaling in the dPAG has been shown to regulate autonomic activity in stress pathways. The same circuitry could also play a role in the setting of baseline autonomic activity and heart rate, according to the ongoing level of stress. The effects of endocannabinoids are many and complex, due, in part, to the widespread distribution of their receptors. As research into endocannabinoid modulation of localized neurocircuitry continues, it is likely to reveal such novel modulatory functions in diverse physiological systems.

ACKNOWLEDGMENTS

The authors thank Victoria Woyach, Erin Koester and Claudia Hermes for their excellent technical expertise.

GRANTS

This work was supported by Merit Review Award no. BX001863 from the U.S. Department of Veterans Affairs Biomedical Laboratory Research and Development Program (to Q. H. Hogan) and by the Research and Education Component of the Advancing a Healthier Wisconsin Endowment at the Medical College of Wisconsin (to C. J. Hillard).

REFERENCES

1. Batkai S, Pacher P, Osei-Hyiaman D, Radaeva S, Liu J, Harvey-White J, Offertaler L, Mackie K, Rudd MA, Bukoski RD, Kunos G. Endocannabinoids acting at cannabinoid-1 receptors regulate cardiovascular function in hypertension. Circulation. 2004; 110:1996–2002. [PubMed: 15451779]
2. Benowitz NL, Jones RT. Cardiovascular and metabolic considerations in prolonged cannabinoid administration in man. J Clin Pharmacol. 1981; 21(8–9 Suppl.):214S–223S. [PubMed: 6271827]
3. Benowitz NL, Rosenberg J, Rogers W, Bachman J, Jones RT. Cardiovascular effects of intravenous delta-9-tetrahydrocannabinol: autonomic nervous mechanisms. Clin Pharmacol Ther. 1979; 25:440–446. [PubMed: 428189]
4. Blankman JL, Simon GM, Cravatt BF. A comprehensive profile of brain enzymes that hydrolyze the endocannabinoid 2-arachidonylglycerol. Chem Biol. 2007; 14:299–315.
5. Bowles NP, Hill MN, Bhagat SM, Karatsoreos IN, Hillard CJ, McEwan BS. Chronic non-invasive glucocorticoid administration suppresses limbic endocannabinoid signaling in mice. Neuroscience. 2012; 204:83–89. [PubMed: 21939741]
6. Brown Brenowitz SDSP, Regehr WG. Brief presynaptic bursts evoke synapse-specific retrograde inhibition mediated by endogenous cannabinoids. Nat Neurosci. 2003; 6:1048–1057. [PubMed: 14502290]
7. Castillo PE, Younts TJ, Chavez AE, Hashimotodani Y. Endocannabinoid signaling and synpatic function. Neuron. 2012; 76:70–81. [PubMed: 23040807]
8. Cravatt BF, Demarest K, Patricelli MP, Bracey MH, Giang DK, Martin BR, Lictman AH. Supersensitivity to anandamide and enhanced endogenous cannabinoid signaling in mice lacking fatty acid amide hydrolase. Proc Natl Acad Sci USA. 2001; 98:9371–9376. [PubMed: 11470906]
9. Cravatt BF, Giang DK, Mayfield SP, Boger DL, Lerner RA, Gilula NB. Molecular characterization of an enzyme that degrades neuromodulatory fatty-acid amides. Nature. 1996; 384:83–87. [PubMed: 8900284]
10. Dampney RAL, Furlong TM, Horiuchi J, Iigaya K. Role of dorsolateral periaqueductal gray in the coordinated regulation of cardiovascular and respiratory function. Auton Neurosci. 2013; 175:17–25. [PubMed: 23336968]
11. Dalton VS, Zavitsanou K. Cannabinoid effects on CB_1 receptor density in the adolescent brain: An autoradiographic study using the synthetic cannabinoid HU210. Synapse. 2010; 64:845–854. [PubMed: 20842718]
12. Dean C. Cannabinoid and GABA modulation of sympathetic nerve activity and blood pressure in the dorsal periaqueductal gray of the rat. Am J Physiol Regul Integr Comp Physiol. 2011; 301:R1765–R1772. [PubMed: 21940402]
13. Dean C. Endocannabinoid modulation of sympathetic and cardiovascular responses to acute stress in the periaqueductal gray of the rat. Am J Physiol Regul Integr Comp Physiol. 2011; 300:R771–R779. [PubMed: 21228344]
14. Dean C, Coote JH. Discharge patterns in postganglionic neurones to skeletal muscle and kidney during activation of the hypothalamic midbrain defence areas in the cat. Brain Res. 1986; 77:271–278.
15. Dean C, Seagard JL, Hopp FA, Kampine JP. Differential control of sympathetic activity to kidney and skeletal muscle by ventral medullary neurons. J Auton Nerv Syst. 1992; 37:1–10. [PubMed: 1593089]
16. Devane WA, Hanus L, Breuer A, Pertwee RG, Stevenson LA, Griffin G, Gibson D, Mandelbaum A, Etinger A, Mechoulam R. Isolation and structure of a brain constituent that binds to the cannabinoid receptor. Science. 1992; 258:1946–1949. [PubMed: 1470919]

17. Di Marzo V, Melck D, Bisogno T, De Petrocellis. Endocannabinoids: endogenous cannabinoid receptor ligands with neuromodulatory action. Trends Neurosci. 1998; 21:521–528. [PubMed: 9881850]
18. Duarte JMN, Nogueira C, Mackie K, Oliveira CR, Cunha RA, Kofalvi. Increase of cannabinoid CB_1 receptor density in the hippocampus of streptozotocin-induced diabetic rats. Exp Neurol. 2007; 204:479–484. [PubMed: 17222407]
19. Eckberg DL. Sympathovagal balance. A critical appraisal. Circulation. 1997; 96:3224–3332. [PubMed: 9386196]
20. Galiègue S, Mary S, Marchand J, Dussossoy D, Carrière D, Carayon P, Bouaboula M, Shire D, Le Fur G, Casellas P. Expression of central and peripheral cannabinoid receptors in human immune tissues and leukocyte subpopulations. Eur J Biochem. 1995; 232:54–61. [PubMed: 7556170]
21. Gemes G, Rigaud M, Dean C, Hopp FA, Hogan QH, Seagard JL. Baroreceptor reflex is suppressed in rats that develop hyperalgesia behavior after nerve injury. Pain. 2009; 146:293–300. [PubMed: 19729245]
22. Hillard CJ. The endocannabinoids signaling system in the CNS: A primer. Int Rev Neurobiol. 2015; 125:1–47. [PubMed: 26638763]
23. Hilton SM, Redfern WS. A search for brain stem cell groups integrating the defence reaction in the rat. J Physiol. 1986; 378:213–228. [PubMed: 3795103]
24. Ho WS, Hillard CJ. Modulators of endocannabinoid enzymic hydrolysis and membrane transport. Hand Exp Pharmacol. 2005; 168:187–207.
25. Huestis MA, Gorelick DA, Heishman SJ, Preston KL, Nelson RA, Moolchan ET, Frank RA. Blockade of effects of smoked marijuana by the CB_1-selective cannabinoid receptor antagonist SR141716. Arch Gen Psychiatry. 2001; 58:322–328. [PubMed: 11296091]
26. Ising M, Holsboer F. Genetics of stress responses and stress-related disorders. Dialogues Clin Neurosci. 2006; 8:433–444. [PubMed: 17290801]
27. Janhayala BS, Hamed AT. Pulmonary and systemic hemodynamic effects of Δ9-tetrahydrocannabinol in conscious and morphine-chloralose-anesthetized dogs: Anesthetic influence on drug action. Eur J Pharmacol. 1978; 53:63–68. [PubMed: 738360]
28. Keay KA, Bandler R. Parallel circuits mediating distinct emotional coping reactions to different types of stress. Neurosci Biobehav Rev. 2001; 25:669–678. [PubMed: 11801292]
29. Kim J, Alger BE. Reduction in endocannabinoid tone is a homeostatic mechanism for specific inhibitory synapses. Nat Neurosci. 2010; 13:592–600. [PubMed: 20348918]
30. Klumpers LE, Fridberg M, de Kam ML, Little PB, Jensen NO, Kleinloog HD, Elling CE, van Gerven JM. Peripheral selectivity of the novel cannabinoid receptor antagonist TM38837 in healthy subjects. Br J Clin Pharmacol. 2013; 76.6:846–857. [PubMed: 23601084]
31. Kreitzer FR, Stella N. The therapeutic potential of novel cannabinoid receptors. Pharm Ther. 2009; 122:83–96.
32. Lake KD, Martin BR, Kunos G, Varga K. Cardiovascular effects of anandamide in anesthetized and conscious normotensive and hypertensive rats. Hypertension. 1997; 29:1204–1210. [PubMed: 9149688]
33. Lam W, Louis WJ, Verberne AJ. Effect of dorsal periaqueductal gray lesion on baroreflex and cardiovascular response to air-jet stress. J Auton Nerv Syst. 1995; 53:35–42. [PubMed: 7673600]
34. Leman S, Dielenberg RA, Carrive P. Effect of dorsal periaqueductal gray lesion on cardiovascular and behavioural responses to contextual conditioned fear in rats. Behav Brain Res. 2003; 143:169–176. [PubMed: 12900043]
35. Malinowska B, Kwolek G, Göthert M. Anandamide and methanand-amide induce both vanilloid VR1-and cannabinoid CB_1 receptor-mediated changes in heart rate and blood pressure in anaesthetized rats. Naunyn Schmiedebergs Arch Pharmacol. 2001; 364:562–569. [PubMed: 11770012]
36. Malliani A, Pagani M, Lombardi F, Cerutti S. Cardiovascular neural regulation explored in the frequency domain. Circulation. 1991; 84:482–492. [PubMed: 1860193]
37. Manders WT, Vatner SF. Effects of sodium pentobarbital anesthesia on left ventricular function and distribution of cardiac output in dogs, with particular reference to the mechanism for tachycardia. Circ Res. 1976; 39:512–517. [PubMed: 963835]

38. McEwen BS. Physiology and neurobiology of stress and adaptation: Central role of the brain. Physiol Rev. 2007; 87:873–904. [PubMed: 17615391]
39. Mechoulam R, Ben-Shabat S, Hanus L, Ligumsky M, Kaminski NE, Schatz AR, Gopher A, Almog S, Martin BR, Compton DR. Identification of an endogenous 2-monoglyceride, present in canine gut, that binds to cannabinoid receptors. Biochem Pharmacol. 1995; 50:83–90. [PubMed: 7605349]
40. Morita H, Nishida Y, Uemura N, Hosomi H. Efect of pentobarbital anesthesia on renal sympathetic nerve activity in the rabbit. J Auton Nerv Syst. 1987; 20:57–64. [PubMed: 3655183]
41. Mukhopadhyay P, Batkai S, Rajesh M, Czifra N, Harvey-White J, Hasko G, Zsengeller Z, Gerard NP, Liaudet L, Kunos G, Pacher P. Pharmacological inhibition of CB_1 cannabinoid receptor protects against doxorubicin-induced cardiotoxicity. J Am Coll Cardiol. 2007; 50:528–536. [PubMed: 17678736]
42. Niederhoffer N, Szabo B. Cannabinoids cause central sympathoexcitation and bradycardia in rabbits. J Pharmacol Exp Ther. 2000; 294:707–713. [PubMed: 10900251]
43. Osgood PF, Howes JF. Δ^9-tetrahydrocannabinol and dimethylheptylpyran induced tachycardia in the conscious rat. Life Sci. 1977; 21:1329–1335. [PubMed: 927033]
44. Pacher P, Batkai S, Kunos G. The endocannabinoid system as an emerging target of pharmacotherapy. Pharmacol Rev. 2006; 58:389–462. [PubMed: 16968947]
45. Padley JR, Li Q, Pilowsky PM, Goodchild AK. Cannabinoid receptor activation in the rostral ventrolateral medulla oblongata evokes cardiorespiratory effects in anaesthetized rats. Br J Pharmacol. 2003; 140:384–394. [PubMed: 12970095]
46. Patel S, Rademacher DJ, Hillard CJ. Differential regulation of the endocannabinoids anandamide and 2-arachidonylglycerol within the limbic forebrain by dopamine receptor activity. J Pharmacol Exp Ther. 2003; 306:880–888. [PubMed: 12808005]
47. Patel S, Wohlfeil ER, Rademacher DJ, Carrier EJ, Perry LJ, Kundu A, Falck Nithipatikom KJR, Campbell WB, Hillard CJ. The general anesthetic propofol increases brain N-arachidonylethanolamine (anandamide) content and inhibits fatty acid amide hydrolase. Br J Pharmacol. 2003; 139:1005–1013. [PubMed: 12839875]
48. Patel S, Roelke CT, Rademacher DJ, Cullinan WE, Hillard CJ. Endocannabinoid signaling negatively modulates stress-induced activation of the hypothalamic-pituitary-adrenal axis. Endocrinology. 2004; 145:5431–5438. [PubMed: 15331569]
49. Patel S, Carrier EJ, Ho WS, Rademacher DJ, Cunningham S, Reddy DS, Falck JR, Cravatt BF, Hillard CJ. The postmortal accumulation of brain N-arachidonylethanolamine (anandamide) is dependent upon fatty acid amide hydrolase activity. J Lipid Res. 2005; 46:342–349. [PubMed: 15576840]
50. Pfitzer T, Niederhoffer N, Szabo B. Central effects of the cannabinoid receptor agonist WIN55212-2 on respiratory and cardiovascular regulation in anaesthetized rats. Br J Pharmacol. 2004; 142:943–952. [PubMed: 15226190]
51. Rademacher DJ, Meier SE, Shi L, Ho WS, Jarrahian A, Hillard CJ. Effects of acute and repeated restraint stress on endocannabinoid content in the amygdala, ventral striatum, and medial prefrontal cortex in mice. Neuropharmacology. 2008; 54:108–116. [PubMed: 17675104]
52. Sampaio KN, Mauad H, Biancardi VC, Barros JL, Amaral FT, Schenberg LC, Vasquez EC. Cardiovascular changes following acute and chronic lesions of the dorsal periaqueductal gray in conscious rats. J Auton Nerv Syst. 1999; 76:99–107. [PubMed: 10412833]
53. Sugiura T, Kondo S, Sukagawa A, Nakane S, Shinoda A, Itoh K, Yamashita A, Waku K. 2-Arachidonoylglycerol: a possible endogenous cannabinoid receptor ligand in brain. Biochem Biophys Res Commun. 1995; 215:89–97. [PubMed: 7575630]
54. Stern JA. The biology of human variation. Ann NY Acad Sci. 1966; 134:1018–1027.
55. Strougo A, Zuurman L, Roy C, Pinquier JL, van Gerven JM, Cohen AF, Schoemaker RC. Modelling of the concentration—effect relationship of THC on central nervous system parameters and heart rate—insight into its mechanisms of action and a tool for clinical research and development of cannabinoids. J Psychopharmacol (Oxf). 2008; 22:717–726.

56. Tsou K, Nogueron MI, Muthian S, Sanudo-Pena MC, Hillard CJ, Deutsch DG, Walker JM. Fatty acid amide hydrolase is located preferentially in large neurons in the rat central nervous system as revealed by immunohistochemistry. Neurosci Lett. 1998; 254:137–140. [PubMed: 10214976]

57. Van Sickle MD, Duncan M, Kingsley PJ, Mouihate A, Urbani P, Mackie K, Stella N, Makriyannis A, Piomelli D, Davison JS, Marnett LJ, Di Marzo V, Pittman QJ, Patel KD, Sharkey KA. Identification and functional characterization of brainstem cannabinoid CB_2 receptors. Science. 2005; 310:329–332. [PubMed: 16224028]

58. Varga K, Lake K, Huangfu D, Guyenet PG, Kunos G. Mechanism of hypotensive action of anandamide in anesthetized rats. Hypertension. 1996; 28:682–686. [PubMed: 8843898]

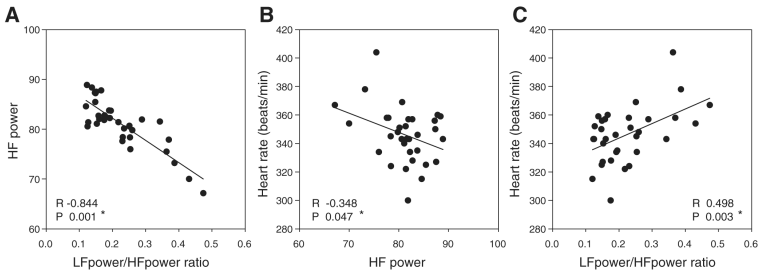

Fig. 1.

Low-frequency (LF) power and LF/high-frequency (HF) power ratio based on heart rate variability (HRV) analysis show a significant inverse correlation (*A*). Baseline heart rate shows a significant negative correlation to HF power, an indicator of parasympathetic tone (*B*), and a significant correlation with the ratio of LF/HF power, an indicator of sympathovagal balance (*C*) ($n = 34$).

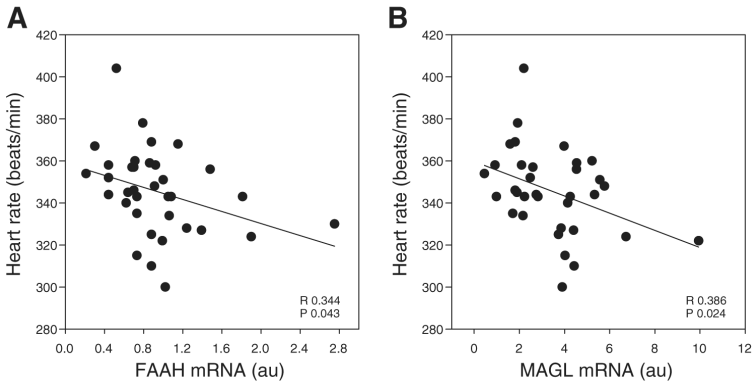

Fig. 2.

Linear regression analysis shows a significant inverse correlation between baseline heart rate and levels of fatty acid amide hydrolase (FAAH; *A*) and monoacylglycerol (MAGL; *B*) mRNA transcript in the dorsal periaqueductal gray ($n = 34$).

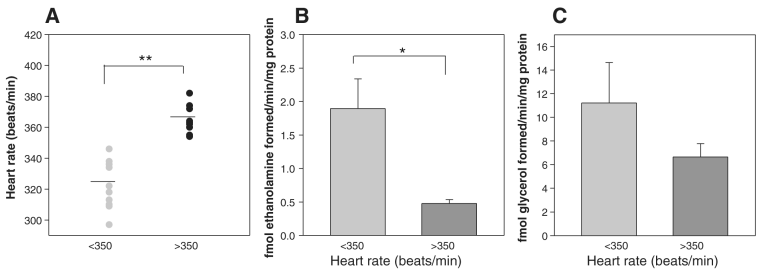

Fig. 3.

Endocannabinoid catabolic enzyme activity in the dPAG. Animals were assigned to low heart rate (<350 beats/min; mean 321; $n = 9$) and high heart rate (>350 beats/min; mean 364; $n = 8$) groups (*A*) for enzyme assay of FAAH (*B*) and MAGL (*C*) activity. FAAH activity in the dPAG was significantly lower in the high heart rate group vs. the low heart rate group, while MAGL activity was unchanged. *$P < 0.001$. **$P < 0.002$.

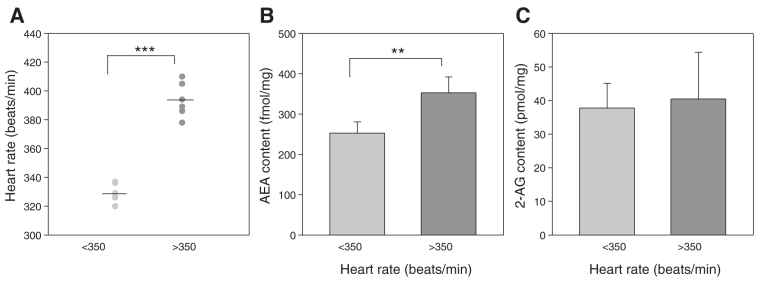

Fig. 4.

Endocannabinoid content in the dPAG. Animals were assigned to low heart rate (<350 beats/min; mean 330; $n = 4$) and high heart rate (>350 beats/min; mean 394; $n = 6$) groups (*A*), for mass spectrometry measurement of anandamide (AEA) (*B*) and 2-arachidonoylglycerol (2-AG) (*C*) content. Anandamide content in the dPAG was significantly higher in the high heart rate group vs. the low heart rate group, while 2-AG content was unchanged. $^{**}P < 0.002$.

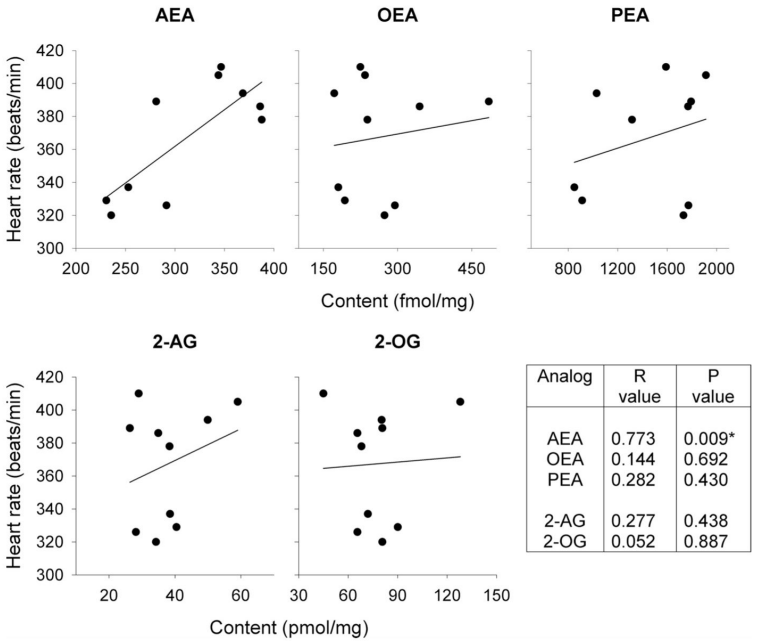

Analog	R value	P value
AEA	0.773	0.009*
OEA	0.144	0.692
PEA	0.282	0.430
2-AG	0.277	0.438
2-OG	0.052	0.887

Fig. 5.

Linear regression analysis demonstrates a significant correlation between baseline heart rate and anandamide (AEA) content, but no correlation with *N*-oleoylethanolamine (OEA), *N*-palmitoylethanolamine (PEA), 2-arachidonoylglycerol (2AG) or 2-oleoyl[3H]glycerol (2-OG) content in the dPAG.

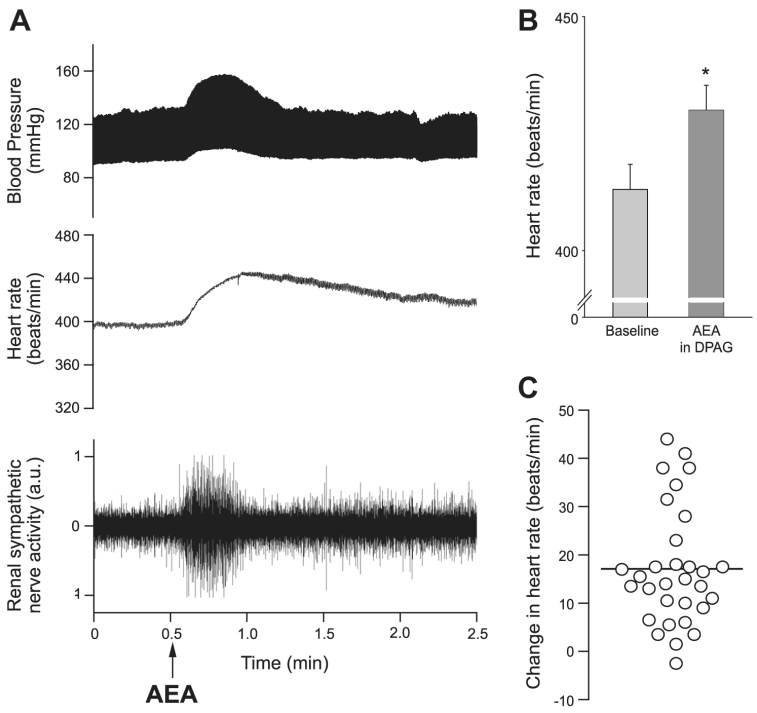

Fig. 6.

An increase in heart rate accompanies pressor and sympathoexcitatory responses evoked by anandamide microinjection (35 nl; 1.75 pmol) into the dPAG (*A*). The peak heart rate response to anandamide is significantly higher than baseline ($P = 0.03$) (*B*), and the range of the increases in heart rate for individual animals is illustrated in *C*, with the bar indicating a mean increase of 17 beats/min.

Table 1

Correlation coefficient R values for dPAG transcript levels of FAAH, MAGL, and CB_1R versus cardiovascular components

	FAAH mRNA				MAGL mRNA				CB_1R mRNA			
	HR	**LF/HF**	**HF**	**BP**	**HR**	**LF/HF**	**HF**	**BP**	**HR**	**LF/HF**	**HF**	**BP**
R Value	−0.344	−0.339	0.357	0.098	−0.386	−0.185	0.270	0.090	0.082	−0.198	0.164	−0.146
P Value	0.043 *	0.050 *	0.038 *	0.581	0.024 *	0.294	0.122	0.614	0.657	0.278	0.371	0.424

* Level of significance set at $P \leq 0.05$.